Revue des Energies Renouvelables Vol. 18 N°2 (2015) 329 – 345
DOI: https://doi.org/10.54966/jreen.v18i2.510

Photogeneration and excitons distribution function in organic bulk heterojunction solar cells

Irénée Vianou Madogni [1,3*], Basile Bruno Kounouhéwa [2,3] and Cossi Norbert Awanou [3†]

[1] Ecole Doctorale Sciences des Matériaux, EDSM
Université d'Abomey-Calavi, UAC/FAST, Bénin, République du Bénin
[2] Centre Béninois de la Recherche Scientifique et Technique, CBRST 03
03 B.P. 1665 Cotonou, République du Bénin
[3] Laboratoire de Physique du Rayonnement, LPR, FAST-UAC 01
01 B.P. 526 Cotonou, République du Bénin

(reçu le 15 mars 2015 – accepté le 17 Juin 2015)

Abstract - *In this work, the excitons distribution function in organic bulk heterojunction solar cells, at a depth* z *has been determined from solving the charge continuity equation, by exploiting the Laplace transform with an appropriate boundary conditions. Next, the influence of the electron-hole pair separation distance on the excitons dissociation probability, the internal quantum efficiency and the binding energy, has been studied. The simulated results show that the probability density of the carriers photogenerated depend on the generation rate, excitons dissociation and the charge carriers in the cells. The potential improvement of the internal quantum efficiency of charge generation depends on electron-hole pair separation distance, the excitons dissociation probability into free charges and depends strongly on the optical absorption of the photons in the active layer.*

Résumé - *Dans ce travail, la fonction de distribution des excitons dans les cellules solaires organiques à hétérojonction volumique, à une profondeur* z *a été déterminée à partir de la résolution de l'équation de continuité de charge, en exploitant la méthode de transformée de Laplace avec une condition aux limites appropriées. Ensuite, l'influence de la distance de séparation de la paire électron-trou sur la probabilité de dissociation des excitons, le rendement quantique interne et l'énergie de liaison a été étudié. Les résultats simulés montrent que la densité de probabilité des porteurs photogénérés dépendent du taux de génération, la dissociation des excitons et les porteurs de charge dans les cellules. L'amélioration potentielle de l'efficacité quantique interne de génération de charge, dépend de la distance de séparation de la paire électron-trou, de la probabilité de dissociation des excitons en charges libres et dépend fortement de l'absorption optique des photons dans la couche active.*

Mots clés: Fonction de distribution - Excitons - Transformée de Laplace – Photo génération de charges - Rendement quantique interne - Probabilité de dissociation.

1. INTRODUCTION

The active layer of organic solar cells is based on the concept of donor-acceptor heterojunction introduced by Tang [1] to create a better charge separation. This layer is a blend of an electrons donor (D) and an electrons acceptor (A). The most studied system which is referenced in an organic solar cells, is regioregular poly(3-hexylthiophene) (rrP_3HT) (electron donor) blended with [6,6]-phenyl C_{61}-butyric acid methyl ester(PCBM) (electron acceptor) (rrP_3HT-PCBM) [2, 3]. The area of the interface between the donor and the acceptor is enhanced and efficient exciton

* ivianou@yahoo.fr - kbbasile@gmail.com
† cawanou@yahoo.fr

dissociation can generate a higher short circuit current density J_{sc} and a net increasing in the internal quantum efficiency [4]. Although the bulk heterojunction blend has been introduced to improve the device performance, the power conversion efficiency of polymer solar cells is still very low.

This energy conversion efficiency of about 10.7 % obtained by Heliatek and Green *et al.* [5, 6], reached the high power conversion efficiency of 12 % recently, obtained on a standard size of 1:1 cm^2 combining two different absorbing materials [7]. These materials generate a high recovery photons, dramatically improving the energy conversion efficiency through a higher photo voltage signal in cells.

The electronic and optical properties such as; the efficiency of photon absorption, the exciton dissociation rate and geminate recombination, exciton diffusion length and non geminate bimolecular recombination can play important roles on the performance of organic bulk heterojunction solar cells [8]. The hightest occupied molecular orbital (HOMO) of the donor and the lowest unoccupied molecular orbital (LUMO) of the acceptor can limit the open circuit voltage V_{oc}, the short circuit current density J_{sc} and therefore the efficiency of the device [9-11]. Better performances of solar cells based on P_3HT-PC60BM have been obtained by increasing the regioregularity of P_3HT [12, 13]. This improvement is explained by increasing the value of the internal quantum efficiency (IQE) due to greater absorption near infra-red.

Considerable interest for an improvement to the quantum efficiency conversion by incorporating plasmonic nanoparticles (NPs in active layer of organic solar cells has been showed experimentally [14-18]. The results obtained reveal that the bulk heterojunction can be blend with plasmonic nanoparticles (NPs), which is a new composite material with new optical and electronic properties in the organic solar cells.

To determine the optical propagation in the organic solar cells, the transfer matrix method based on Maxwell's equations is used by considering optical absorption of plasmonic active layers [19]. In order to obtain the electromagnetic field $E(z)$ distribution at a depth z in the cell, the optical transfer-matrix theory (TMF) has been used. The light is treated as a propagating plane wave, which is transmitted and reflected on the interface. The complex reflection r_{ii} and transmission t_{ii} coefficients for a propagating plane wave along the surface normal between two adjacent layers j and k have been determined from Fresnel's theory by considering the effect of optical interference [20]. All these research have been experimentally based on the optical properties of the charge photo generation.

Recently, in order to understand the origin of the phenomena of surface losses, Yang *et al.* (2012) have defined quantitatively and calculated the loss probability of free charge carriers at the metal/organic (M/O) interfaces from numerical simulations [21]. They have found that the origin of surface losses is the free charge carrier extraction from the wrong electrodes, or the direct extraction or surface recombination of pair polaron without dissociation.

De Falco *et al.* (2012) for high lighting the role of the exciton dynamics in determining the transient activation time in organic photovoltaic devices, they carried out a temporal semi-discretization using an implicit adaptive method for the numerical treatment [22]. The resulting sequence of differential sub problems has been linearized using the Newton Raphson method with inexact Jacobian and exponentially fitted finite elements for spatial discretization.

However, there is very little theoretical works on the distribution theory of the phenomenon of the charge photo generation and the excitons profile in organic bulk

heterojunction solar cells. Moreover, charge photo generation phenomenon, transport phenomenon, recombination and excitons dissociation into-free-charge, the surface loss of free charge carriers at the metal/organic (M/O) interface are important processes in the organic solar cells.

The objective of this paper is to study theoretically the photogeneration and excitons distribution function in the organic bulk heterojunction solar cells in order to understand the excitons dynamics in the cells. The charge continuity equation has been solved using Laplace transform and the residue theorem. Next, the influence of the Coulomb interaction between the electron and hole on the dissociation probability, the internal quantum efficiency, the binding energy distribution and efficiency of the excitons absorption have been analyzed and interpreted. The simulated results have been compared with those existing in the literature [20-22].

The paper is organized as following: in Section 2, the architecture of the organic bulk heterojunction solar cell considered is described. Subsequently, a theoretical approach of the generation mechanism, recombination and dissociation of excitons in free charge carriers and excitons transport are presented. An overview of relevant equations and the solving of the charge continuity equation are shown. The simulated results and discussion are presented in Sections 3. Finally, the conclusion and outlook are listed in Section 4.

2. MATERIAL AND METHOD

2.1 Architecture of the organic solar cell

The structure of the solar cell considered, is blend of ITO/PEDOT:PSS/rrP_3HT: PC70BM (1:0.7 weight ratio)/Yb/Al. The layer Yb/Al is cathode and ITO/PEDOT:PSS is anode. Ytterbium limit electrochemistry between aluminum and sulfur of P_3HT in film and allows improvement of open circuit voltage, shunt resistance and fill factor (FF) [23].

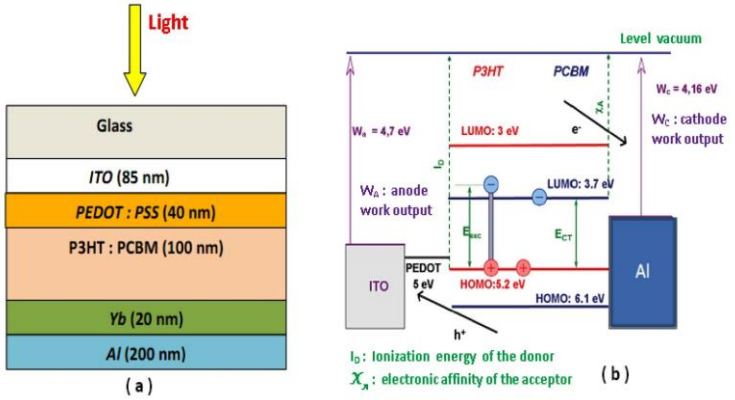

Fig. 1: **a-** Ideal structure of the cell, **b-** band diagram of the cell ITO/PEDOT/ rrP_3HT:PCBM /Yb/Al [26]

The BHJ blend is represented by the HOMO and LUMO levels of the donor and acceptor. The band offset between the LUMO levels of donor and acceptor guarantees the charge separation at the interface if the lifetime of the exciton is sufficiently long to meet a split site as shown in figure 1.

The choice of donor-acceptor pair defines the alignment of electronic levels of the system. This alignment is important because the energy difference between the HOMO

of the donor and the LUMO of the acceptor is directly linked to the potential V_{oc} of the solar cell while the energy difference between the LUMO of the two materials ensures exciton dissociation [24, 25].

The blend rrP_3HT:PC70BM is chosen to indicate the interest of complementary absorption of PC70BM in active layer [26].

2.2 Excitons generation

The quantity energy of incident light absorbed by active layer of a organic solar cell depends on the complex index of refraction $\bar{n} = n + iK$ of donor-acceptor materials [20]. The average energy dissipated per second for a given wavelength λ of incident light at the position z in the organic film can be calculated by:

$$Q(z,\lambda) = \frac{1}{2} c \varepsilon_0 \alpha_j n \left| \bar{E}(z) \right|^2 \tag{1}$$

where, c, is the vacuum speed of light, ε_0, the permittivity of vacuum, n, the real index of refraction, $\alpha = \frac{4k\Pi}{\lambda}$, the absorption coefficient, and $E(z)$, the electrical optical field at point z, $Q(z,\lambda)$ have the unit of W/m^3 [27, 28].

Assuming that every photon generates one exciton, the exciton generation rate at position z in the material is:

$$G(z,\lambda) = \frac{Q(z,\lambda)}{h\nu} = \frac{\lambda Q(z,\lambda)}{hC} \tag{2}$$

where h, is Planck constant, ν, is the frequency of incident light. We have modeled frequency $G(z,\lambda)$ by {Eq. (3)}:

$$G(z,\lambda) = \alpha L_0 \exp\left(-\frac{1}{L} z \right) = G_0 \exp(-\alpha z) \tag{3}$$

where $G_0 = \alpha I_0$ is the generation rate of singlet excitons depending of the incident light intensity. L, is the exciton diffusion length and α, the absorption coefficient [29, 30].

2.3 Generation and excitons recombination

In organic bulk heterojunction semiconductors, the mechanism of recombination is Langevin-type controlled by the mobility of the charge carriers [30-32]. The charge continuity equation is expressed as followed,

$$\begin{cases} -\frac{1}{q}\frac{dJ_n(z)}{dz} + P.G(z) - (1-P)R(z) = 0 \\ -\frac{1}{q}\frac{dJ_p(z)}{dz} + P.G(z) - (1-P)R(z) = 0 \end{cases} \tag{4}$$

with q, the elementary charge, $J_n(z)$ et $J_p(z)$, the electron and hole current density at a depth z in the active layer, $G(z)$, the photon absorption rate, P, the dissociation probability of charge carrier pair and $R(z)$, the bi-molecular recombination rate from Langevin model is,

$$R(z) = \left[n(z).p(z) - n_i^2 \right] (\mu_n + \mu_p) \frac{q}{\varepsilon_r . \varepsilon_0} \tag{5}$$

where $n(x)$, electron density, $p(z)$, hole density, n_i, intrinsic carrier density, μ_n, electron mobility, μ_p, hole mobility and ε_r et ε_0, spatial average static permittivity of active layer respectively [31, 32].

$$\begin{cases} J_n(z) = -qn(z)\times\mu_n E(z) + qD_n\dfrac{dn(z)}{dz} \\ J_p(z) = -qp(z)\times\mu_p E(z) - qD_p\dfrac{dp(z)}{dz} \end{cases} \quad (6)$$

$D_{n,p}$, are the carrier diffusion coefficients given by the Einstein relation:

$$D_{n,p} = \mu_{n,p}\, k_B \frac{T}{q} \quad (7)$$

where k_B is the Boltzmann constant and T : the absolute temperature.

The electric field distribution $E(z)$ is determined by the Poisson equation.

$$\frac{dE(z)}{dz} = \frac{q}{\varepsilon_r.\varepsilon_0}(n(z) - p(z)) \quad (8)$$

The built-in voltage V_{bi} is determined by,

$$\int_0^{L'} E(z)\,dz = V_{ap} - V_{bi} \quad (9)$$

where V_{ap}, the external applied voltage and L', the active layer thickness [33 - 35].

To find the exciton distribution, the continuity equation can be applied with a one dimensional diffusion model for exciton movement, the generation rate from {Eq. (1)} and recombination in the bulk becomes,

$$D\frac{\partial^2 P}{\partial z^2} - \frac{D.P}{L^2} + G = 0 \quad (10)$$

where P, the excitons distribution, D excitons diffusion constant, L, diffusion length.

Boundary conditions must be chosen to solve {Eq. (10)} in each layer.

$$D\frac{\partial P}{\partial z}\bigg|_{z=z0} = S\,.\,p(z_0) \quad (11)$$

where $z = z_0$ at the interface, and S is the interfacial exciton-quenching velocity. S describes the recombination of excitons at the interface, and $S = 0$ corresponds to no recombination while $S = \infty$ corresponds to complete quenching at the interface [29]. The Laplace transform is used to solve {Eq. (10)} with the residue theorem.

2.4 Resolution of charge continuity equation

The solution of {Eq. (10)} is obtained by determining its image using the residue theorem,

(i) First case: let us assume that $G(z,\lambda) = G_0 = cste$

The Laplace transform gives: $£[G(z,\lambda] = G_0/P$

The image of {Eq.(10)} is obtained by posing $X = P$ and $Y = Sp(z_0) = Cste \neq G_0$.

$$X = \frac{L^2(-G_0 + Sp(z_0)P^2}{Dp(L^2p^2 - 1)} \quad (12)$$

The original of {Eq. (12)} solution of {Eq. (10)} given the excitons distribution function in the cell,

$$P(z) = \frac{L^2 G_0}{D} + \frac{L^2}{2D}\left(-L^2 G_0 + S_p(z_0)\right) \times \cosh\left(\frac{z}{L}\right) \quad (13)$$

(ii) Second case: $G = f(z)/G(z,\lambda) = G_0 \exp(-az)$

The Laplace transform gives: $£[G(z,\lambda] = \frac{G_0}{p+\alpha}$

The image of {Eq. (10)} is obtained,

$$X = \frac{L^2 Sp(z_0)p}{D(L^2p^2 - 1)} - \frac{L^2 G_0}{D(p+\alpha).(L^2p^2 - 1)} \quad (14)$$

The original of {Eq. (14)}, solution of {Eq. (10)} gives the excitons distribution function in the organic cell,

$$P(z_0) = \frac{L^2 G_0}{D(1 - L^2\alpha^2)} e^{-\alpha z} + \left(\frac{L^2 Sp(z_0)}{D} - \frac{L^4 G_0}{D(1 - L^2\alpha^2)}\right) \cosh\left(\frac{z}{L}\right) \quad (15)$$

(iii) Third case: we took into account, the excitons field dependent mobility then we have, $G(z,\lambda) = (1 - e^{-\gamma z})$ with $\gamma = L_G / L_D$, where L_G, excitons generation length, L_D, excitons dissociation length.

The Laplace transform is expressed as followed: $£[G(z,\lambda] = \frac{1}{p} - \frac{1}{p+\gamma}$

The image of {Eq. (10)} is given by,

$$X = \frac{L^2 Sp(z_0)p}{D(L^2p^2 - 1)} - \frac{L^2\gamma}{Dp(p+\gamma).(L^2p^2 - 1)} \quad (16)$$

The original of {Eq. (16)}, solution of {Eq. (10)} gives the excitons distribution function in the original solar cell according to the residue theorem.

$$P(z_0) = \frac{L^2}{D} - \frac{L^2}{D(1 - L^2\gamma^2)} e^{-\alpha z} + \left(\frac{L^2 Sp(z_0)}{2D} - \frac{L^6\gamma^2}{D(1 - L^2\gamma^2)}\right) \cosh\left(\frac{z}{L}\right) \quad (17)$$

2.5 Generation and excitons dissociation into-tree-charge carriers

The photon absorption by an organic material generates in the majority of cases an exciton of Frenkel-type. These excitons photo generated, not all of them can be dissociated into-free carriers. In our numerical simulation, the field dependency of charges generation is processed by the Onsager-Braun model which gives the probability of electron-hole pair dissociation [36-39]:

$$P(E,T) = \frac{K_D(E,T)}{K_D(E,T) + K_F} \quad (18)$$

K_F, is the rate of charge transfer recombination and K_D is the dissociation rate of a bound electron-hole pair:

$$K_D(E,T) = K_R \frac{3}{4\Pi a^3} \exp\left(-\frac{U_B}{K_B T}\right) \frac{J_1\left(2\sqrt{-2b(E,T)}\right)}{\sqrt{-2b(E,T)}} = \frac{3}{4\Pi a^3} \exp\left(-\frac{U_B}{K_B T}\right) \left[1 + b + \frac{b^2}{3} + ...\right] \quad (19)$$

where a, the electron-hole separation distance, U_B, electron-hole pair binding energy described as $U_B = \frac{q^2}{4\Pi \varepsilon_0 \varepsilon_r a}$, $b = \frac{q^3 E}{8\Pi \varepsilon_0 \varepsilon_r K_B^2 T^3}$, T, the temperature, E, the electric field, ε_r, the dielectric constant of the material, ε_0, spatial permittivity, $K_R = \frac{q}{\varepsilon}(\mu_n + \mu_p)$, the bimoleculare recombination rate of Langevin and J_1 is the Bessel function of order. $\frac{1}{\eta} = \exp\left(-K\frac{\sqrt{E}}{K_B T}\right)$ is the efficiency of dissociation given by Onsager-Braun [36, 37] where $K = \sqrt{\frac{e^3}{\Pi \varepsilon \varepsilon_0}}$

Taking into account the disorder in the blend, a distribution of the excitons probability having different separation distances have been incorporated into the numerical simulations [37, 38]. As a result, {Eq. (18)} should be integrated over a distribution of separation distances,

$$P(a,T,E) = \int_0^\infty p(z,T,E) \,.\, f(a,z)\,dz \quad (20)$$

Where, $f(a,z)$ is a normalized distribution function given by,

$$f(a,z) = \frac{4}{a^3\sqrt{\Pi}} z^2 \exp\left(-\frac{z^2}{a^2}\right) \quad (21)$$

$p(E,T,z)$ is the dissociation probability at a specific distance z I, an organic solar cell. The procedure used for the numerical simulations has been described in detail by [40].

2.6 Generation and excitons transport

Charge transport in the organic solar cells device is governed by the set of continuity equations [21, 40-44],

$$\begin{cases} \frac{\partial n(z)}{\partial t} - \mathrm{div} J_n\, z) = G_n - R_n\, n(z) \\ \frac{\partial p(z)}{\partial t} - \mathrm{div} J_p\, z) = G_p - R_p\, p(z) \end{cases} \quad (22)$$

where n and p, electrons and holes density, J_n et J_p, electrons and holes flux density, G_n et G_p, charge carriers generation rate, $J = q(J_p - J_n)$, the total current density, $R_n n$ and $R_p p$, electrons and holes recombinaison rate.

The charge carriers flux density is given by,

$$\begin{cases} J_n(z) = -q\mu_n n(z) E(z) + \mu_n KT\, \partial n(z)/\partial z \\ J_n(z) = -q\mu_p n(z) E(z) - \mu_p KT\, \partial p(z)/\partial z \end{cases} \quad (23)$$

where E, electric field, μ_n and μ_p, the charge carriers mobility and the electric field distribution $E(z)$ is determined by the Poisson equation {Eq. (8)},

$$\frac{\partial E(z)}{\partial z} = \frac{q}{\varepsilon_r . \varepsilon_0}\left(n(z) - p(z)\right) \quad (24)$$

We denote by $X(z)$ the volume density of geminate pairs and we express its rate of charge as,

$$\frac{\partial X(z)}{\partial t} = G(z,t) + \gamma pn - (k_{diss} + k_{rec})X(z) \quad (25)$$

where (k_{diss}), dissociation constant, (k_{rec}), recombination constant, $G(z,t)$, the speed at which excitons reach interfaces and partially separated, (γpn), the speed at which free electrons and holes are attracted to each other and recombine, γ, Langevin constant.

Boundary and initial conditions

$n(z,0) = n_0(z)$, $p(z,0) = p_0(z)$ and $X(z,0) = X_0(z)$ are needed to complete the model.

At the interface $\partial X/\partial t = 0$, therefore $\frac{\partial n}{\partial t} = \frac{\partial p}{\partial t} = 0$

The {Eq. (22)} and {Eq. (25)} become,

$$X(z) = \tau G + \gamma \tau p(z) n(z) \quad (26)$$

where, $\tau = 1/k_{diss} + k_{rec}$

$$\begin{cases} -\mathrm{div} J_n(z) = G_n - R_n n(z) \\ -\mathrm{div} J_p(z) = G_p - R_p p(z) \end{cases} \quad (27)$$

After substituting {Eq. (27)} into {Eq. (10)} and imposes to {Eq. (23)}, the condition, $\left.\frac{\partial n(z)}{\partial z}\right|_{z=0,L} = \left.\frac{\partial p(z)}{\partial z}\right|_{z=0,L} = 0$ and $\frac{\partial J_n}{\partial z} = 0$, we have,

$$\begin{cases} D_n \frac{\partial^2 P_n}{\partial z^2} - \frac{D_n . P_n}{L_n^2} + R_n n = 0 \\ D_p \frac{\partial^2 P_p}{\partial z^2} - \frac{D_p . P}{L_p^2} + R_p p = 0 \end{cases} \quad (28)$$

The Laplace transform gives the images of {Eq. (28)} for the electrons and holes

$$X_n = \frac{L_n^2\left(-R_n n + Y . D_n . p_n^2\right)}{p_n(L_n^2\, p_n^2 - 1)} \quad (29)$$

$$X_p = \frac{L_p^2\left(-R_p p + Y . D_p . p_p^2\right)}{p_p(L_p^2\, p_p^2 - 1)} \quad (30)$$

The originals of {Eq. (29)} and {Eq. (30)} solution of {Eq. (28)} gives the distribution function of the electrons and holes,

$$P_n(z) = R_n n L_p^2 + \frac{L_n^3}{2}\left(-R_n n + \frac{Sp(z_0)D_n}{L_n^2}\right)\cosh\left(\frac{z}{L_n}\right) \tag{31}$$

$$P_p(z) = R_p p L_p^2 + \frac{L_p^3}{2}\left(-R_n p + \frac{Sp(z_0)D_p}{L_p^2}\right)\cosh\left(\frac{z}{L_p}\right) \tag{32}$$

The excitons distribution function in the cell is given by the relation,

$$p(z) = p_n(z) + p_p(z) \tag{33}$$

Taking into account the absorption coefficients α_1 and α_2 of the donor and acceptor ($\frac{\partial J_n}{\partial z} \neq 0$ and $\frac{\partial J_p}{\partial z} \neq 0$), the current density distribution function for the electrons $J_n(z)$ and holes $J_p(z)$ are given by,

$$J_p(z) = \frac{q\alpha_1 L_p(1-R)}{(\alpha_1^2 L_p^2 - 1)}\left(\frac{\left(\frac{SL_p}{D_p} + \alpha_1 L_p - Y + \sinh\frac{z}{L_p}\right)}{\left(\frac{SL_p}{D_p}\sinh\frac{z}{L_p} + \cosh\frac{z}{L_p}\right)} - \varphi\right) \tag{34}$$

$$J_p = \frac{q\alpha_2 L_n(1-R)\vartheta}{(\alpha_1^2 L_p^2 - 1)}\left(\alpha_2 L_n - \frac{\left(\frac{SL_n}{D_n}\cosh\frac{z}{Ln} - + \exp-\alpha_2 z + \phi\right)}{\left(\frac{SL_n}{D_n}\sinh\frac{z}{L_n} + \cosh\frac{z}{L_n}\right)}\right) \tag{35}$$

Where,

$$\varphi = \alpha_1 L_p \exp(-\alpha_1 z)$$

$$\phi = \sinh\left(\frac{z}{L_n}\right) + \alpha_2 L_n \exp(-\alpha_2 z)$$

$$\vartheta = \left(\exp(-\alpha_1(z + L_p))\exp(-\alpha_2 L_n)\right)$$

$$Y = \exp(-\alpha_1 z)\left(\frac{SL_p}{D_p}\cosh\left(\frac{z}{L_p}\right)\right)$$

The excitons photogenerated distribution function in the active layer is given by,

$$J(z) = q(1-R) \times \exp(-\alpha_1 z)\,(1 - \exp(-\alpha_1 L_p - -\alpha_2 L_n)) \tag{36}$$

3. RESULTS AND DISCUSSION

3.1 Excitons distribution function in the cell

Parameters used in the device model simulations; $a = 1.8\,\text{nm}$, electron-hole separation distance in the CT state, $G_0 = 6\times10^{27}\,\text{m}^{-3}\text{s}^{-1}$, optical generation rate, $T = 300\,\text{K}$, the temperature, $E_g = 1.7\,\text{eV}$, effective band gap of P_3HT and 2.4 ev,

effective band gap of PCBM, the mobilities of holes and electrons in P_3HT:PCBM (1:0.7 by weight) are $10^{-3}cm^2V^{-1}s^{-1}$ and $2:10^{-3}$- $4:5:10^{-3}cm^2V^{-1}s^{-1}$, $\varepsilon_r = 3.4$, relative dielectric constant, $L=10nm$, length diffusion, $D=7.2\times10^{-20}m^2/s$, constant diffusion; $K_R \approx 4\times10^8$, recombination rate and $K_D \approx 4\times10^7$, dissociation rate, $\tau=6.2\times10^{-7}s$, effective lifetime, $S=0.2cm^2$, device area, $I_{irr}=I_0=100mW/cm^2$, $J_{sc}=8.31\ mAcm^2$, short circuit current density, $V_{oc}=0.58V$, open circuit voltage, $V_{bi}=0.54$, built-in voltage, $R_s=12.38\ \Omega.cm^2$, series resistance, $R_p=1.76\ k\Omega.cm^2$, shunt resistance, $FF=50.3\%$, fill factor, $\eta=2.43\%$, power conversion efficiency and the voltage applied to the cell is between -0.54V et 0:54V, $L_n=10nm$, the electrons diffusion length, $L_p=1nm$, the holes diffusion length, $G_n=1.5\times10^{27}m^{-3}s^{-1}$, the electrons generation rate, $G_p=1.5\times10^{27}m^{-3}s^{-1}$, the holes generation rate, $D_n=5.2\times10^{-27}m^2s^{-1}$, the electrons diffusion constant, $D_p=2.6\times10^{-7}m^2s^{-1}$, the holes diffusion constant, $\alpha_1=\alpha_2=2\times10^5cm^{-1}$, absorption coefficient of electrons and holes, $L_G=75cm$, the excitons generation length, $L_D=150cm$, excitons dissociation length and $\gamma=5\times10^{-3}cm^{0.5}s^{-0.5}$, field dependent mobility parameter.

The figure 2 and figure 3 show the evolution of excitons distribution function as a function of the organic layer thickness. They are obtained for $G_0 = 6\times10^{27}\ m^{-3}s^{-1}$, $L = 10\ nm$, $D=7.2\times10^{-20}\ m^2s^{-1}$, $p(z_0)=1$ and $S = 0.2\ cm^2$. The figure 2 is obtained from {Eq. (13)} after resolution of {Eq. (10)} where the excitons generation rate is constant in the cell and the figure 3 is obtained from {Eq. (15)} after resolution of {Eq. (10)} where the excitons generation rate is modeled by $G(z_0,\lambda) = G_0 \exp(-\alpha z)$.

We first note that the distribution remains constant whatever the variation of the organic thickness layer. Next, it decreases linearly with an abrupt variation of the organic layer thickness.

This linear decreasing is due to the excitons loss mobility in the cell; there are drift of charges. This factor can be attribute to the loss of free charge carriers at the electrodes/organic (M/O) interfaces. It causes an increasing of the interfacial dissociation rate and a diffusivity of the electron-hole pair at D/A interface. This result has been obtained by Yang *et al.* [21].

The opposite phenomenon is observed on figure 3 where the excitons photogenerated are dissociated normally at D/A interface for being collected at the electrodes. When the mobility parameter of the excitons is considered, we obtained the same results as shown in {Eq. (17)} that those obtained in the case of the figure 3.

Therefore, this result reveals that the mobility coefficient is not more important parameter which influence the optoelectronic properties in the organic photovoltaic devices. Which confirms the validity of our model.

3.2 Excitons generation rate distribution in the active layer

Considering the organic layer as an homogeneous material, the simulated results show that the excitons generation rate decreases with the increasing of the active layer

thickness as described in {Eq. (3)} which makes the corresponding average exciton generation rate (total exciton generation rate divided by the thicknes) become smaller.

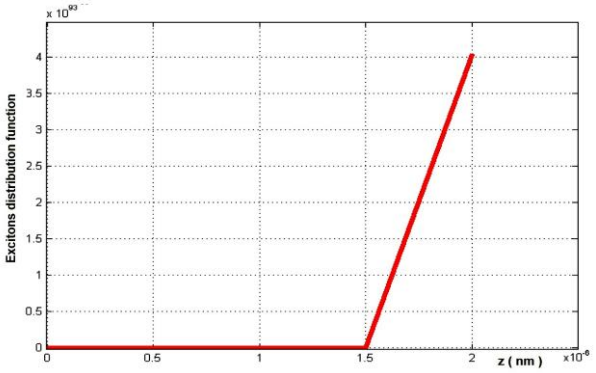

Fig. 3: Excitons distribution function as function of the organic layer thickness

However, when we took into account the excitons mobility, on remarked that, at the initial stage, the average exciton generation rate increases with the increasing thickness of the active layer as shown in figure 4. With the further increase of the active layer, the average generation rate becomes larger and decreases very rapidly although other photo-generation peaks appear in the active layer as shown in figure 5. This is because the absolute values for the peaks become small, which leads to the corresponding decrease of average exciton generation rate.

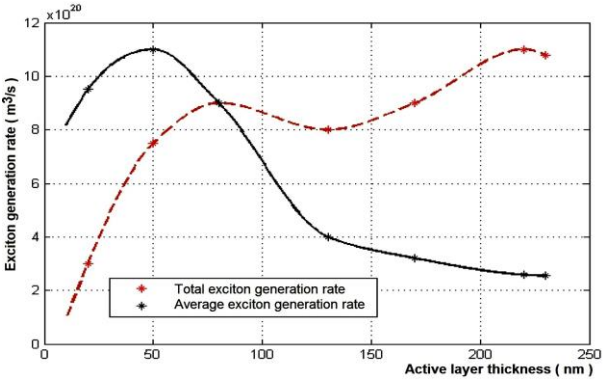

Fig. 4: The calculated exciton generation rate in the active layer

Moreover, when the active layer thickness increases from 20 to 50 nm, the total excitons generation rate increases from to 3×10^{27} to 7.5×10^{27} $m^{-3}s^{-1}$. This rate decreases very slightly from 9×10^{27} to 8×10^{27} $m^{-3}s^{-1}$ with the increasing of the active layer between 70 and 130 nm and increases again with the further increase of the active layer.

Whereas we remarked the net increasing of average exciton generation rate between 9.5×10^{27} and 8×10^{27} $m^{-3}s^{-1}$ with the increasing of the active layer from 20 to 50 nm, which decrease very rapidly and reaches a rate from 2.56×10^{27} $m^{-3}s^{-1}$ with the further increases of the active layer. As a result, when the active layer thickness increase, the excitons generation rate increase.

This result reveals the increasing of the photons absorption rate and the excitons mobility rate in the active layer. This result has been proved theoretically by De Falco *et al.* [22] and experimentally predicted by Zhang *et al.* [20] considering the optical interference effect in the active layer.

3.3 Current density distribution function in the active layer

The figure 5 shows the current density J_{SC} distribution function of the excitons photogenerated in the active layer. It represents the curve obtained from {(Eq. (36)} after substituting {(Eq. (34)} and {(Eq. (35)} into {(Eq. (22)}.

The figure 6 revealed that, when the active thickness increases from 20 to 80 nm, J_{SC} reaches its maximum value, and followed by a little decrease until 145 nm and increases again until 225 nm and behaves wavelike. When the thickness increases further, J_{SC} increases again. Which reveals that J_{SC} should be proportional to the total exciton generation rate and all the excitons photo generated can be dissociated into free charge carriers and then collected by the electrodes.

Moreover, when the active layer thickness increases, J_{SC} increases and unfortunately, there is obvious deviation between our results and prediction. This deviation is due to the low excitons dissociation probability rate into free charge carriers with the increasing of the active layer thickness. These results have been obtained experimentally by [26, 20]. Obviously, the assumption that the exciton-to-free-carrier dissociation probability is unity is not totally correct.

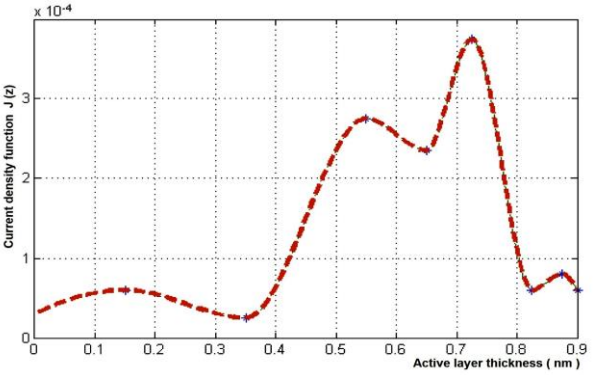

Fig. 5: Current density function as a function of the active layer thickness

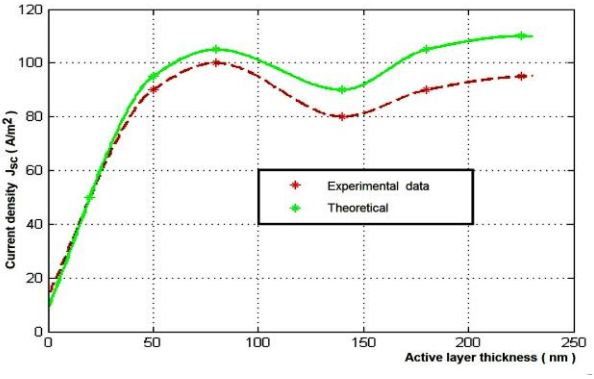

Fig. 6: Density current as a function of the active layer thickness

3.4 Distribution of internal quantum efficiency - Excitons dissociation probability

The figure 7 and 8 translated the internal quantum efficiency distibution (IQE) and excitons dissociation probability respectively as a function of a specific distance z in

the organic layer. When the electron-hole separation distance " a " increases, the excitons dissociation probability decreases and the internal quantum efficiency increase which considerably improves the current density in the cell. This result reveal, a feeble Coulomb interaction between the electron and hole, a decreasing of the supplemental strength for dissociate the excitons by heat-energy at ambient temperature, a low exciton binding energy and a drop in internal electric field. In this work, a = 0.92 nm as shown in figure 8 gives a better excitons dissociation for a probability equal to unity and for the values of " a " greater than 2 nm, the excitons dissociation into-free-charge carriers is very feeble. Therefore the electron-hole separation distance is a key parameter for an effective dissociation of the excitons at D/A interface.

We determined the distribution function of the excitons binding energy (U_b) and external quantum efficiency (EQE) as a function of the photons absorption energy by varying the electron-hole pair separation distance " a " (Fig. 9). The simulated results reveal that when the photons energy increases, the binding energy decreases. This behavior confirms the previous results as shown in figure 7 and figure 8. Furthermore, the Coulomb attraction and the exchange energy dramatically depend on the separation distance between electron and hole. Experimental results show that the exchanged energy for the intramolecular excitonic states is around 0:7 eV [45]. For the cases of polaron pair state and charge-transfer complex state, the situation would be different mainly due to the electron hole pair separation distance.

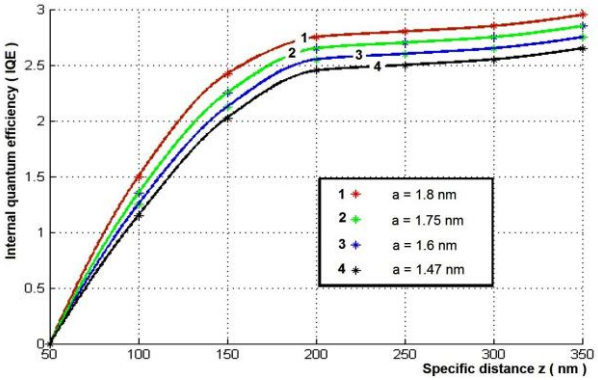

Fig. 7: Internal quantum efficiency (IQE) as a function of the organic layer thickness

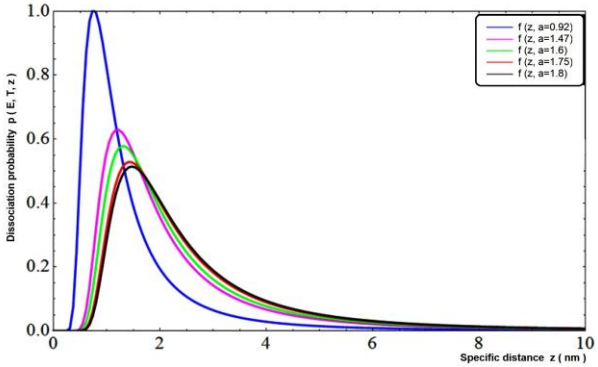

Fig. 8: Excitons dissociation probability at a specific distance z in the organic layer

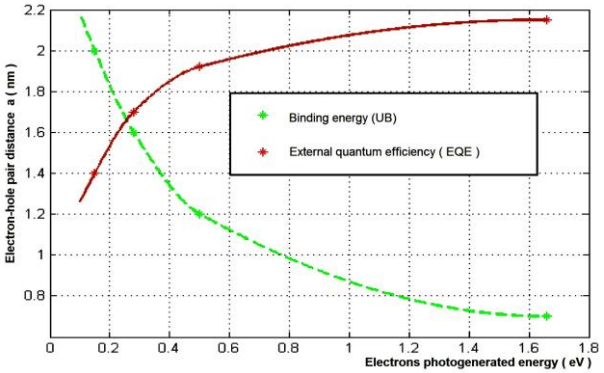

Fig. 9: Distribution function of the excitons binding energy (UB) and external quantum efficiency (EQE) as a function of the photons absorption energy

4. CONCLUSION AND OUTLOOK

We determined the excitons distribution function in an organic bulk heterojunction solar cell ITO/PEDOT: PSS/rrP_3HT: PC70BM (1: 0.7 weight ratio)/Yb/Al using the Laplace transforms with the residue theorem. The influence of the electron-hole pair separation distance on the excitons dissociation probability, the quantum efficiency of charge carriers generation, the current density photo-generated and on the excitons binding energy have been studied.

The simulated results indicate that the linear decreasing of the excitons generation function is attributed to the loss of free charge carriers at the electrodes/organic (M/O) interfaces. It causes the increasing of the interfacial dissociation rate and a diffusivity of the electron-hole pair at D/A interface. We remarked that the total exciton generation rate does not monotonous ly increases with the increasing of the active layer thickness, but behaves wavelike which induces the corresponding variation of J_{SC}. The carrier lifetimes also influence J_{SC} greatly. When the lifetimes of both electrons and holes are long enough, dissociation probability plays an important role for the thick active layer. J_{SC}. Behaves wave like with the variation of the active layer thickness. In addition the excitons dissociation probability decreases exponentially when the electron-hole pair separation distance increases and the internal quantum efficiency charge generation monotonously increases.

Our results are in agreement with those predicted by the literature. Moreover, the phenomena of charge generation and the excitons dissociation into-free-charge carriers are important processes in organic bulk heterojunction solar cells. The potential improvement of the internal quantum density of charge generation depends on the exciton dissociation probability into-free-charge carriers and strongly depends on the photons optical absorption.

Future work can be about (i) extensions to the model; (ii) improvement of the analytical results and (iii) the model study as a stochastic processes using Fokker Planck equations.

ACKNOWLEDGEMENTS

We thank Dr. B.M. Agbomahéna, Dr. M. Ossénath, Dr. K. N'Gobi Gabin and Dr. J. Doumatè for reading the manuscript. We acknowledge the financial supports by the Trading Company

SOCOMA-Bénin, and 'Ecole Doctorale Sciences des Matériaux (EDSM)' and 'Laboratoire de Physique du Rayonnement LPR, FAST-UAC 01BP 526 Cotonou République du Bénin'

REFERENCES

[1] C.W. Tang and S.A. VanSlyke, '*Organic Electroluminescent Diodes*', Applied Physics Letters, Vol. 51, N°12, pp. 913 – 915, 1987.

[2] J.S. Kim, J.H. Park, J.H. Lee, J. Jo, D.Y. Kim, and K. Cho, '*Control of the Electrode Work Function and Active Layer Morphology Via Surface Modification of Indium Tin Oxide for High Efficiency Organic Photovoltaic's*'. Applied Physics Letters, Vol. 91, N°11, 112111-3, 2007.

[3] M. Arnaud, Ph.D. Thesis, University of Montréal, 2012.

[4] G. Yu, J. Gao, J.C. Hummelen, F. Wudl and A. J. Heeger, '*Polymer Photovoltaic Cells: Enhanced Efficiencies via a Network of Internal Donor-Acceptor Heterojunctions*', Science, Vol. 270, N° 5243, pp. 1789 - 1791, 1995.

[5] Heliatek, http://www.heliatek.com//*p=1923lang=en avril 2012*

[6] M.A. Green, Y.H. K. Emery, W. Warta and E.D. Dunlop, '*Program Photovoltaics 20*', 2012.

[7] www.enerzine.com

[8] C.J. Brabec, M. Heeney, I. Mcculloch and J. Nelson, '*Influence of Blend Microstructure on Bulk Heterojunction Organic Photovoltaic Performance*', Chemical Society Reviews, Vol. 40, N°3, pp. 1185 – 1199, 2011.

[9] A.C. Mayer, S.R. Scully, B.E. Hardin, M.W. Rowell and M.D. Mcgehee, '*Polymer-based Solar Cells*', Materials Today, Vol. 10, N°11, pp. 28 – 33, 2007.

[10] C.F.N. Marchiori and M. Koehler, '*Dipole Assisted Exciton at Conjugated/Fullerene Photovoltaic Interfaces: A Molecular Study Using Density Functional Theory Calculations*' Synthetic Metals, Vol. 160, N°7-8, pp. 643 – 650, 2010.

[11] M.C. Scharber, D. Möuhlbacher, M. Koppe, P. Denk, C. Waldauf, A.J. Heeger and C.J. Brabec, '*Design Rules for Donors in Bulk-Heterojunction Solar Cells - Towards 10% Energy-Conversion Efficiency*', Advanced Materials, Vol. 18, pp. 789-794, 2006.

[12] F. Zhang, M. Johansson, M.R. Andersson, J.C. Hummelen and O. Inganäs, '*Polymer Photovoltaic Cells with Conducting Polymer Anodes*', Advanced Materials, Vol. 14, N°9, pp. 662 - 665, 2002.

[13] T. Kugler and W.R. Salaneck, '*Chemical Species at Polymer/ITO Interfaces: Consequences for the Band Alignment in Light-Emitting Devices*', Comptes Rendus de l'Académie des Sciences, Séries IV Physics, Vol. 1, N°4, pp. 409 – 423, 2000.

[14] A.P. Kulkarni, K.M. Noone, K. Munechika, S.R. Guyer and D.S. Ginger, '*Plasma-Enhanced Charge Carrier Generation in Organic Photovoltaic Films using Silver Nano prisms*', Nano Letters, Vol. 10, N°4, pp. 1501 – 1505, 2010.

[15] M. Xue, L. Li, B.J.T. De Villers, H. Shen, J. Zhu, Z. Yu, A.Z. Stieg, Q. Pei, B.J. Schwartz and K.L. Wang, Applied Physics Letters, Vol. 98, N°25, pp. 253302, 2010.

[16] D.H. Wang, D.Y. Kim, K.W. Choi, J.H. Seo, S. H. Im, J.H. Park, O.O. Park and A.J. Heeger, '*Enhancement of Donor-Acceptor Polymer Bulk Heterojunction Solar Cell Power Conversion Efficiencies by Addition of Au Nanoparticles*', Angewandte Chemie International Edition, Vol. 50, N°24, pp. 5519 – 5523, 2011.

[17] C.C.D. Wang, W.C.H. Choy, C. Duan, D.S. Dixon Fung, E.I. Wei, F.X. Sha, F.X. Xie, F. Huang and Y. Cao, '*Optical and Electrical Effects of Gold Nanoparticles in the Active Layer of Polymer Solar Cells*', Journal of Materials Chemistry, Vol. 22, pp. 1206 - 1211, 2012.

[18] J. Zhu, M. Xue, R. Hoekstra, F. Xi, B. Zenga and K.L. Wang, '*Light Concentration and Redistribution in Polymer Solar Cells by Plasmonic Nanoparticles*', Nanoscale, Vol. 4, pp. 1978 - 1981, 2012.

[19] M. Born and E. Wolf, '*Principles of Optics: Electromagnetic Theory of Propagation, Interference and Diffraction of Light*', 7th edition, Cambridge University Press, Cambridge, UK, 1999.

[20] C. Zhang, H. You, Y. Hao, Z. Lin and C. Zhu, '*Inverted Organic Photovoltaic Cells with Solution-Processed Zinc Oxide as Electron Collecting Layer*', Japanese Journal of Applied Physics, Vol. 50, 082302, 2011.

[21] W. Yang, D Li Li, Y. Yao, X. Hou and C.Q. Wu, '*Enhanced Surface Losses of Organic Solar Cells Induced by Efficient Polaron Pair Dissociation at the Metal/Organic Interface*', Journal of Applied Physics, Vol. 112, N°3, pp. 034510-034510-7, 201).

[22] C. de Falco, R. Sacco and M. Verri, 'Analytical and Numerical Study of Photocurrent Transients In Organic Polymer Solar Cells, 'math.NA' 2012.

[23] C. Waldauf, P. Schilinsky, M. Perisutti, J. Hauch and C.J. Brabec, '*Solution-Processed Organic n-Type Thin-Film Transistors*', Advanced Materials, Vol. 15, N°24, pp. 2084 - 2088, 2003.

[24] F. Monestier, J.J. Simon, Ph. Torchio, L. Escoubas, F. Flory, S. Bailly, R. de Bettignies, S. Guillerez, and C. Defranoux, '*Modeling the Short Circuit Current Density of Polymer Solar Cells Based on P3HT:PCBM Blend*', Solar Energy Materials and Solar Cells, Vol. 91, N°5, pp. 405 – 410, 2007.

[25] D.J. Servaites, M.A. Ratner and T.J. Marks, '*Organic Solar Cells: A New Look at Traditional Models*', Energy & Environmental Science, Vol. 4, N°11, pp. 4410 – 4422, 2011.

[26] M.B. Agbomahéna, Ph.D. Thesis, cotutelle between University de Mons (Belgique) and University d'Abomey-Calavi (Bénin), N°26, 2013.

[27] L.A.A. Perttersson, L.S. Roman and O. Inganäs, '*Modeling Photocurrent Action Spectra of Photovoltaic Devices Based on Organic thin Film*', Journal of Applied Physics, Vol.86, N°1, pp. 487 – 496, 1999.

[28] S. Yoo, '*Organic Solar Cells Based on Liquid Crystalline and Polycrystalline thin Films*', PhD Dissertation, University of Arizona, Tuscon.

[29] W.J.Jr Potscavage, *Physics and Engineering of Organic Solar Cells*, Georgia Institute of Technology, May 2011.

[30] De-Li Li, Wei Si, Wen-Chao Yang, Yao Yao, Xiao-Yuan Hou, Chang-Qin Wu, '*Spike in Transient Photocurrent of organic Solar Cell: Exciton Dissociation at Interface*', Physics Letters A Vol. 376, N°4, pp. 227 – 230, 2012.

[31] J. Nelson, '*Polymer: Fullerene Bulk Heterojunction Solar Cells*', Materials Today, Vol. 14, N°10, pp. 461 – 470, 2011.

[32] F.C. Spano, J. Clark, C. Silva and R.H. Friend, '*Determining Exciton Coherence from the Photoluminescence Spectral Line Shape in Poly(3-Hexylthiophene) Thin Films'.* Journal of Chemical Physics, Vol. 130, N°7, 074904, 2009.

[33] S.H. Park, A. Roy, S. Beaupré, S. Cho, N. Croates, J.S. Moon, D. Moses, M. Leclerc, K. Lee and A.J. Heeger, '*Bulk heterojunction solar cells with internal quantum efficiency approaching 100&percent*', Nature Photonics, Vol. 3, N°5, pp. 397 – 302, 2009.

[34] M.M. Mandoc, L.J.A. Koster and P.W.M. Blom. '*Optimum Charge Carrier Mobility In Organic Solar Cells*', Applied Physics Letters, Vol. 90, 133504, 2007.

[35] J. Zhu, M. Xue, R. Hoekstra, F. Xiu, B. Zeng and K.L. Wang, '*Light Concentration and Redistribution in Polymer Solar Cells by Plasmonic Nanoparticles*', Nanoscale, Vol. 4, 1978 p., 2012.

[36] L. Onsager, '*Journal of Chemical Physics*', Vol. 2, 599 p., 1934.

[37] C.L. Braun, '*Electric Field Assisted Dissociation of Charge Transfer States as a Mechanism of Photocarrier Production*', Journal of Chemical Physics, Vol. 80, pp. 4157 – 4161, 1984.

[38] P. Peumans, S. Uchida and S.R. Forrest, '*Efficiency Buck Heterojunction Photovoltaic Cells Using Small-Molecular-Weight Organic Thin Films*', Nature, Vol. 425, N°6954, pp. 158 - 162, 2003.

[39] L.J.A. Koster, E.C.P. Smits, V.D. Mihailetchi, and P.W.M. Blom, '*Device Model for the Operation of Polymer/Fullerene Buck Heterojunction Solar Cells*', Physical Review B, Vol. 72, N°8, 2005.

[40] S. Gunes, H. Neugebauer and N. Sariciftci, *'Conjugated Polymer-Based organic Solar Cells*', Chemical Reviews, Vol. 107, N°4, pp. 1324 – 1338, 2007.

[41] J.A. Barker, C.M. Ramsdale and N.C. Greenham, '*Modeling the Current-Voltage Characteristics of Bilayer ¨Polymer Photovoltaic Device*', Physical Review B, Vol. 67, N°7, 2003.

[42] G.A. Buxton and N. Clarke, '*Computer Simulation of Polymer Solar Cells*', Modeling Simulation Materials Science Engineering, Vol. 15, pp. 13 – 26, 2007.

[43] I. Hwang and N.C. Greenham, '*Modelling Photocurrent Transients in Organic Solar Cells*', Nanotechnology, Vol. 19, N°42, pp. =424012, 2008.

[44] S.L.M. van Mensfoort, SIE Vulto, R.A.J. Janssen, R. Coehoorn, '*Hole Transport in Polyfluorene-Based Sandwich-Type Devices: Quantitative Analysis of the Role of Energetic Disorder*', Physics Reviews B, Vol. 78, N°8, 2008.

[45] A. Kohler and D. Beljonne, '*The Singlet-Triplet Exchange Energy in Conjugated Polymers*', Advanced Functional Materials, Vol. 14, N°1, pp. 11 - 18, 2004.